

# Influence of the Oxygen Content, Pressure and Temperature in the API N-80 Corrosion for Applications of CCS-EOR Processes

Juan Orozco-Agamez<sup>a,\*</sup>, Luis F. Santos<sup>a,b</sup>, Julián A. Moreno<sup>a,b</sup>, Anibal Alviz-Meza<sup>a,c</sup>, Adan Y. Leon<sup>a,b</sup>, Darío Pena-Ballesteros<sup>a</sup>

<sup>a</sup> Universidad Industrial Santander, Escuela de Ingeniería Metalúrgica y Ciencia de los Materiales, Grupo de Investigaciones en Corrosión – GIC, cra 27 calle 9, Bucaramanga –Santander, Colombia

<sup>b</sup> Universidad Industrial Santander, Escuela de Ingeniería de Petróleos, Grupo de Recobro Mejorado – GRM, cra 27 calle 9, Bucaramanga –Santander, Colombia

<sup>c</sup> Universidad Señor de Sipán, Facultad de Ingeniería, Arquitectura y Urbanismo, Grupo de investigación en Deterioro de Materiales, Transición energética y Ciencia de Datos DANT3, Km. 5 via Pimentel, Chiclayo, Perú  
[juan.orozco1@correo.uis.edu.co](mailto:juan.orozco1@correo.uis.edu.co)

Enhanced oil recovery in processes involving the presence of carbon dioxide (CO<sub>2</sub>) is the option with the greatest potential for carbon capture and storage (CCS-EOR). The content of molecular oxygen in the flue gas current generates problems and risks associated with corrosion that must be evaluated. Similarly, the analysis of the effects of temperature and working pressure, represent two variables of great interest. In this research, the effects of the variables oxygen removal efficiency, temperature, and pressure, in real conditions of an oil field in Colombia, were evaluated by means of a thermodynamic simulation tool. The presence of the following corrosion products Fe<sub>2</sub>O<sub>3</sub>, Fe<sub>3</sub>O<sub>4</sub>, MnCO<sub>3</sub>, MnO<sub>2</sub>, and FeCO<sub>3</sub> was determined. It was observed that the presence of FeCO<sub>3</sub> and MnCO<sub>3</sub> corrosion products occur only for removal efficiencies equal to or greater than 95%. Temperature has a greater influence on the products formed in equilibrium (Fe<sub>2</sub>O<sub>3</sub>, Fe<sub>3</sub>O<sub>4</sub>, MnCO<sub>3</sub>) at a constant pressure, whereas pressure has a greater influence on MnO<sub>2</sub> and FeCO<sub>3</sub> at a constant temperature.

## 1. Introduction

Carbon dioxide emissions into the atmosphere have reached a maximum of 36 billion tons per year (versus 6 billion tons in 1950). To comply with the Paris Agreement, net greenhouse gas emissions must be zero or even negative by 2050 to keep global warming well below 1.5–2 °C compared to pre-industrial levels (Fernandez, 2022). CO<sub>2</sub> emissions can be reduced through carbon capture and storage. Enhanced oil recovery in processes involving the presence of carbon dioxide (CO<sub>2</sub>) is the option with the greatest potential for carbon capture and storage (CCS-EOR) (Li et al., 2019). Researchers report that injection techniques that use CO<sub>2</sub> to improve oil recovery have become an ideal option due to the possibility of capturing, using, and sequestering CO<sub>2</sub> (Qing et al., 2018).

On the other hand, there are several problems associated with this method (CCS-EOR), including the corrosive effects caused by the deterioration of the materials commonly used in the injection process, such as carbon steels, which are an excellent choice in terms of availability, properties, and cost-benefit ratio (Souza et al., 2020). Authors such as (Nikitasari et al., 2021), indicate that the increase in temperature contributes to the acceleration in the corrosion rate of carbon steel pipe in condensate solution from a geothermal power plant. It has been reported that increases in temperature contributed to the corrosion rate up to a maximum peak, after which, protective films began to form, resulting in a decrease in the corrosion rate (Choi et al., 2017).

Li and collaborators found that corrosion rate decreased due to the formation of protective corrosion layers at higher temperatures (Li et al., 2019). Regarding the oxygen content variable, when assessing the risk of corrosion, it is necessary to know the amount of oxygen that enters to the system (Hagarová et al., 2021). Likewise, the effect of oxygen on the corrosion of carbon steels, and the presence of oxygen could seriously

reduce the protective properties of the oxide scales formed by Fe–Cr alloys at high temperatures (Meng et al., 2022). Studies of corrosion have used simulation as a phase prior to experimentation to obtain the system's behaviour in thermodynamic equilibrium and observe the theoretical corrosion products (Orozco et al., 2018). The present study analyses the effects generated by different oxygen contents in a flue gas-vapor current of a CCS-EOR process under the operating conditions of a Colombian oil field. Additionally, the effects of temperature and pressure on corrosion products are examined. As a result of the analysis of these three independent variables such as the efficiency of oxygen removal, pressure, and temperature considering thermodynamic equilibrium in the process, the idea of working with high oxygen removal efficiencies to develop safer transportation processes can be corroborated.

## 2. Materials and Methods

### 2.1 Study environment and material composition

The study environment was selected from real data of an outlet current of steam generator equipment in a Colombian field. A similar environment was reported in the paper by (Moreno et al., 2021), however, this work considers the presence of oxygen, which occurs in real conditions, given the amount of excess oxygen used in the process (Table 1). The selected study material was API N-80 carbon steel.

Table 1. composition of the environment

Component	O <sub>2</sub>	CO <sub>2</sub>	N <sub>2</sub>	H <sub>2</sub> O
% Mol	1.21	4.31	35.08	59.40

Table 2 reports API N-80 the steel mass composition used as the basis to conduct the simulations in this research work. The steel/gas stream molar ratio used for this simulation was 1/1000. This relationship was selected considering the criteria followed in the research by (Alviz et al., 2018).

Table 2: Chemical composition of the API N-80 grade steel used in the study (Li et al, 2019)

Element	C	S	Si	Mn	P	Cr	V	Fe
% weight	0.35	0.015	0.30	1.45	0.02	0.12	0.11	97.64

### 2.2 Selection of oxygen removal efficiency values and determination of theoretical corrosion products

The study of the removal efficiency on the analysis of the corrosion products formed in equilibrium was conducted at 6 measurement levels (0, 50, 90, 95, 97 and 99%). For the independent variables temperature (520, 540 and 560 °F) and pressure (800, 950 and 1,100 psia), three measurement levels were selected, considering the actual operating conditions in the Colombian field of study.

### 2.3. Effect of temperature and pressure on the amounts formed in equilibrium of the theoretical corrosion products

The equilibrium quantities formed for the main compounds obtained in this research and their variation as a function of each variable were determined.

For this purpose, the variation calculation of the substance's amount formed in equilibrium with respect to the temperature at a constant pressure Eq(1), as well as with respect to the pressure at a constant temperature Eq(2). It presents behavior at a constant temperature of 560°F and a constant pressure of 800 psia, which is consistent with the other study values.

$$\left(\frac{\partial n}{\partial T}\right)_P = \left|\frac{n_2 - n_1}{T_2 - T_1}\right| \quad (1)$$

$$\left(\frac{\partial n}{\partial P}\right)_T = \left|\frac{n_2 - n_1}{P_2 - P_1}\right| \quad (2)$$

Where,

$\left(\frac{\partial n}{\partial T}\right)_P$  and  $\left(\frac{\partial n}{\partial P}\right)_T$ : represent the variation of the substance's amount (kmol) with respect to temperature at constant pressure (kmol/°F) and with respect to pressure at constant temperature (kmol/psia). n: moles at the indicated condition (kmol). T: temperature (°F). P: pressure (psia).

### 3. Results and Discussion

#### 3.1 Effect of the presence of molecular oxygen in the steam-flue gas stream

Theoretical corrosion products in the flue gas-steam stream were determined, considering the percentages of oxygen removal described in section 2.2.

Table 3. Theoretical corrosion products obtained from the O<sub>2</sub> removal efficiency in the steam-flue gas stream

Removal efficiency	Amount of O <sub>2</sub> in the stream (kmol)	Products formed depending on the amount of O <sub>2</sub>			
99%	0.12	Fe <sub>2</sub> O <sub>3</sub>	Fe <sub>3</sub> O <sub>4</sub>	FeCO <sub>3</sub>	MnCO <sub>3</sub>
97%	0.36	Fe <sub>2</sub> O <sub>3</sub>	Fe <sub>3</sub> O <sub>4</sub>	FeCO <sub>3</sub>	MnCO <sub>3</sub>
95%	0.61	Fe <sub>2</sub> O <sub>3</sub>	Fe <sub>3</sub> O <sub>4</sub>	FeCO <sub>3</sub>	MnCO <sub>3</sub>
90%	1.21	Fe <sub>2</sub> O <sub>3</sub>	MnO <sub>2</sub>	-	-
50%	6.07	Fe <sub>2</sub> O <sub>3</sub>	MnO <sub>2</sub>	-	-
0%	12.14	Fe <sub>2</sub> O <sub>3</sub>	MnO <sub>2</sub>	-	-

It was shown that for removal efficiencies greater than 95%, carbonates such as MnCO<sub>3</sub> and FeCO<sub>3</sub> were formed in the material. It has been reported that iron carbonate tends to form a protective layer on the surface of the material (Cui et al., 2019), because it offers a barrier to the interaction between aggressive ions with the metal matrix (Hua et al., 2015).

#### 3.2 Analysis of the removal efficiency, pressure, and temperature with respect to the equilibrium formation of Fe<sub>2</sub>O<sub>3</sub>

Figure 1a describes the effects of molecular oxygen removal efficiency and pressure at a constant temperature of 520 °F. A greater equilibrium amount of Fe<sub>2</sub>O<sub>3</sub> corrosion product is observed for removal efficiencies of 90, 50 and 0 %. An overlapping of the formed equilibrium amounts of corrosion product was evidenced for these three removal efficiencies. Likewise, the behaviour of the formation of the equilibrium quantity for the removal efficiencies with respect to pressure presented a linear behavior, without observing a percentage increase or decrease. The removal efficiency where less equilibrium formation of Fe<sub>2</sub>O<sub>3</sub> was observed was that corresponding to 99%. In this scenario, there was a trend of percentage increase with respect to the pressure variable (800 to 1,100 psia) of 0.20 %. For a removal efficiency of 97 %, a higher equilibrium formation of Fe<sub>2</sub>O<sub>3</sub> was obtained than that observed at a removal efficiency of 99 %. The increase trend observed at this value of efficiency with respect to pressure was 0.18 %. Finally, for the removal efficiency of 95 %, a percentage increase trend of 0.14 % was presented. Figure 1b depicts the effects of molecular oxygen removal efficiency and temperature at constant pressure of 800 psia. As observed in figure 1a, the behavior of the formation of the equilibrium amount of Fe<sub>2</sub>O<sub>3</sub> was higher compared to the efficiencies of 95, 97 and 99 %, likewise, there is an overlap between these removal efficiencies. The behaviour of these removal efficiency values with respect to the formation of the equilibrium amount of Fe<sub>2</sub>O<sub>3</sub> shows a linear behaviour, without observing a percentage increase or decrease

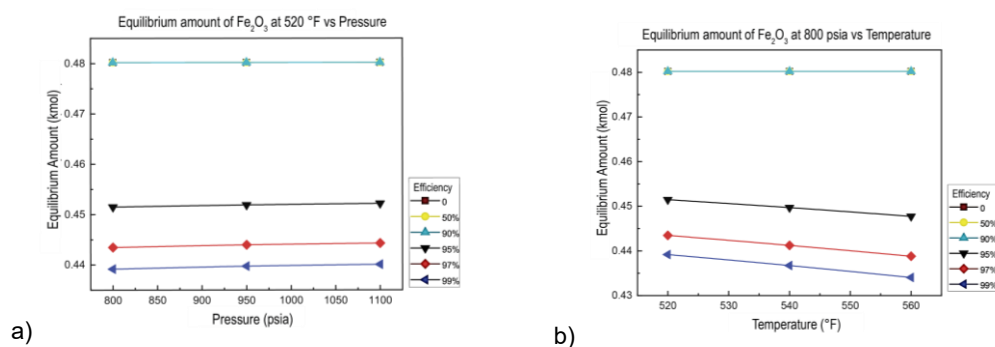


Figure 1: Variation in the equilibrium amount of Fe<sub>2</sub>O<sub>3</sub> at 520 °F with respect to pressure and O<sub>2</sub> removal efficiency. b) Variation in the equilibrium amount of Fe<sub>2</sub>O<sub>3</sub> at 800 psia with respect to temperature and O<sub>2</sub> removal efficiency

The removal efficiency where less equilibrium formation of Fe<sub>2</sub>O<sub>3</sub> was observed was that corresponding to 99 %. In this scenario, a percentage decrease trend was presented with respect to the temperature variable (520

to 560 °F) of 1.16 %. For a removal efficiency of 97 %, a higher equilibrium formation of Fe<sub>2</sub>O<sub>3</sub> was obtained than that observed at a removal efficiency of 99%. The percentage decrease trend observed at this efficiency value with respect to temperature was 1.05 %. Finally, for the removal efficiency of 95 %, a percentage decrease trend of the amount of Fe<sub>2</sub>O<sub>3</sub> formed in equilibrium with respect to temperature of 0.83 % was presented.

**3.3 Analysis of the removal efficiency, pressure, and temperature with respect to the equilibrium formation of Fe<sub>3</sub>O<sub>4</sub> and MnO<sub>2</sub>**

Figure 2a describes the effects of molecular oxygen removal efficiency and pressure at a constant temperature of 520 °F with respect to the equilibrium formation of the corrosion product Fe<sub>3</sub>O<sub>4</sub>. There is no evidence of formation of the study corrosion product when removal efficiencies of 90, 50 and 0 % are present. On the other hand, the removal efficiency where the highest equilibrium formation of Fe<sub>3</sub>O<sub>4</sub> was observed to 99%. In this scenario, a percentage decrease trend was presented with respect to the pressure variable (800 to 1,100 psia) of 7.19 %. For a removal efficiency of 97 %, less equilibrium formation of Fe<sub>3</sub>O<sub>4</sub> was obtained than that observed at a removal efficiency of 99 %. The decrease trend observed at this value of efficiency with respect to pressure was 7.22 %. Finally, for the removal efficiency of 95 %, a percentage decrease trend of 7.30 % was presented. Figure 2b depicts the effects of molecular oxygen removal efficiency and temperature at constant pressure of 800 psia. For the removal efficiency of 99 %, a percentage increase trend was presented with respect to the temperature variable (520 to 560 °F) of 18.79 %. For the removal efficiency of 97 %, a trend of percentage increase with respect to temperature of 19 % was obtained. Finally, for the removal efficiency of 95 %, a percentage increase trend of the amount of Fe<sub>3</sub>O<sub>4</sub> formed in equilibrium with respect to temperature of 19.35 % was presented.

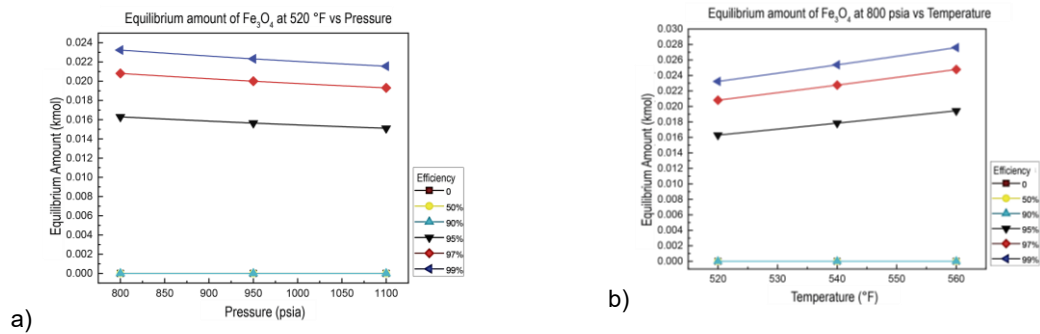


Figure 2. a) Variation in the equilibrium amount of Fe<sub>3</sub>O<sub>4</sub> at 520 °F with respect to pressure and O<sub>2</sub> removal efficiency. b) Variation in the equilibrium amount of Fe<sub>3</sub>O<sub>4</sub> at 800 psia with respect to temperature and O<sub>2</sub> removal efficiency

In contrast to what was observed in the formation of Fe<sub>3</sub>O<sub>4</sub>, there is no evidence of formation of the study corrosion product when removal efficiencies of 99, 97 and 95 % are present. It is important to note that there were percentage decreases in the amount of formation in equilibrium of MnO<sub>2</sub> for the analyzes with respect to the variation in temperature and in the same way with respect to pressure. These percentage decreases for all scenarios were less than 1%. What has been described above is evident in figures 3a and 3b.

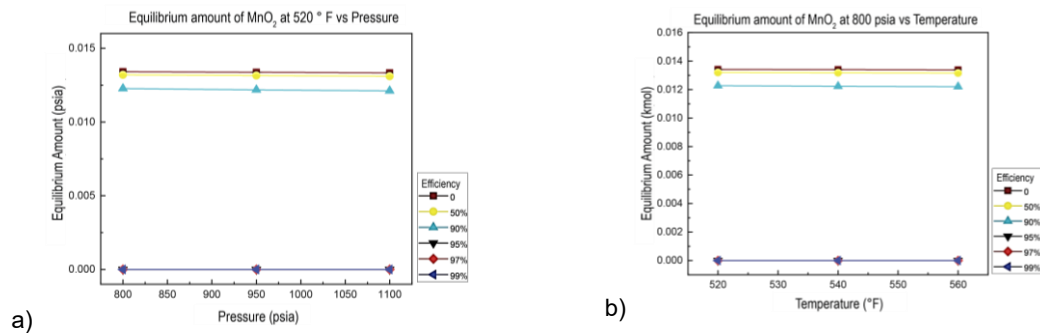


Figure 3. a) Variation in the equilibrium amount of MnO<sub>2</sub> at 520 °F with respect to pressure and O<sub>2</sub> removal efficiency. b) Variation in the equilibrium amount of MnO<sub>2</sub> at 800 psia with respect to temperature and O<sub>2</sub> removal efficiency

### 3.4 Analysis of the removal efficiency, pressure, and temperature with respect to the equilibrium formation of $\text{FeCO}_3$

The effects of molecular oxygen removal efficiency and pressure at a constant temperature of 520 °F can be seen in Figure 4a. No equilibrium amount of  $\text{FeCO}_3$  corrosion product is observed for removal efficiencies of 0, 50 and 90 %. The removal efficiency where the highest equilibrium formation of  $\text{FeCO}_3$  was observed occurred to 99 %. In this scenario, a percentage increase trend was presented with respect to the pressure variable (800 to 1,100 psia) of 26.29 %. For the removal efficiency of 97 %, the percentage increase trend with respect to pressure was 26.27 %. Finally, for the removal efficiency of 95 %, a percentage increase trend of 26.21 % was presented.

Figure 4b depicts the effects of molecular oxygen removal efficiency and temperature at constant pressure of 800 psia. At 99 % removal efficiency, a percentage decrease trend was presented with respect to the temperature variable (520 to 560 °F) of 23.26 %. For the removal efficiency of 97 %, the percentage decrease trend observed was 23.23 %. Finally, for the removal efficiency of 95 %, a percentage decrease trend of the amount of  $\text{FeCO}_3$  formed in equilibrium with respect to temperature of 23.17 % was presented.

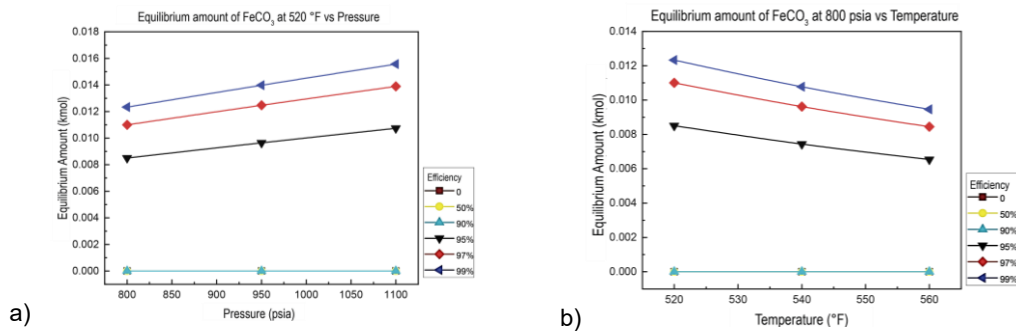


Figure 4. a) Variation in the equilibrium amount of  $\text{FeCO}_3$  at 520 °F with respect to pressure and  $\text{O}_2$  removal efficiency. b) Variation in the equilibrium amount of  $\text{FeCO}_3$  at 800 psia with respect to temperature and  $\text{O}_2$  removal efficiency

### 3.5 Analysis of the removal efficiency, pressure, and temperature with respect to the equilibrium formation of $\text{MnCO}_3$

Figure 5a and 5b describe the effects of molecular oxygen removal efficiency and pressure at a constant temperature of 520 °F with respect to the equilibrium formation of the corrosion product  $\text{MnCO}_3$  and at constant pressure (figure 5b). No equilibrium amount of corrosion product  $\text{MnCO}_3$  is observed for removal efficiencies of 0, 50 and 90 %. Percentage variation of the order of 0.11 % is evidenced for removal efficiencies of 99, 97 and 95%.

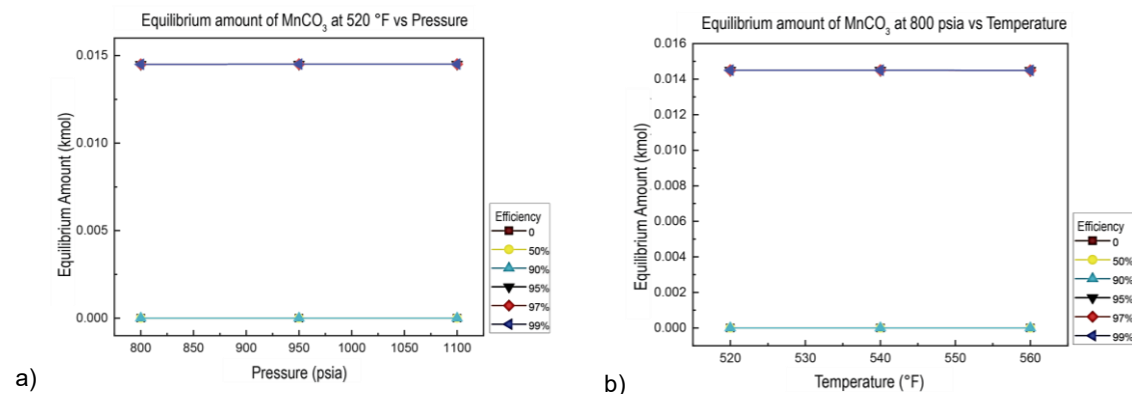


Figure 5. a) Variation in the equilibrium amount of  $\text{MnCO}_3$  at 520 °F with respect to pressure and  $\text{O}_2$  removal efficiency. b) Variation in the equilibrium amount of  $\text{MnCO}_3$  at 800 psia with respect to temperature and  $\text{O}_2$  removal efficiency

#### 4. Conclusions

In this study, the effects of temperature and pressure on corrosion products formed in thermodynamic equilibrium in API N-80 carbon steel material were evaluated using the thermodynamic simulation tool HSC Chemistry in a steam-flue gas environment of a Colombian field. The formation of corrosion products such as  $\text{Fe}_2\text{O}_3$ ,  $\text{Fe}_3\text{O}_4$ ,  $\text{FeCO}_3$ ,  $\text{MnCO}_3$  and  $\text{MnO}_2$  was evidenced.

It was observed that the presence of  $\text{FeCO}_3$ ,  $\text{MnCO}_3$  corrosion products occur only for removal efficiencies equal to or greater than 95 %. Given the protective nature of these corrosion products, especially  $\text{FeCO}_3$ , and taking API N-80 carbon steel as a case study, it is possible to conclude that in the search for safer processes in gas-vapor flow environments, the possibility of removing the molecular oxygen present will be directly related to the formation of products with a passivating characteristic.

In addition, it was possible to establish a greater influence of the temperature variable with respect to the variation of the products formed in equilibrium ( $\text{Fe}_2\text{O}_3$ ,  $\text{Fe}_3\text{O}_4$ ,  $\text{MnCO}_3$ ) and a greater influence of the pressure variable at constant temperature with respect to the variation of the  $\text{MnO}_2$  product. and  $\text{FeCO}_3$ .

#### References

- Alviz A., Sanabria J, Kafarov V, Peña., 2018. Study of Continuous Corrosion on ASTM A335 P91 Steel in an Environment of  $\text{CO}_2$ - $\text{O}_2$ - $\text{N}_2$ - $\text{H}_2\text{O}$  Derived from the Theoretical Combustion Products of a Mixture of Refining Gases at High Temperatures. *Chemical Engineering Transactions*, 70, 1069-1074.
- Choi Y., Hassani S., Nam T., Nestic S., Abas A., Nor A., Suhor M., 2017. Corrosion Inhibition of Pipeline Steels under Supercritical  $\text{CO}_2$  Environment. *CORROSION 2017*, New Orleans, Louisiana, USA.
- Cui G., Yang Z., Liu J., Li Z., 2019. A comprehensive review of metal corrosion in supercritical  $\text{CO}_2$  environment. *International Journal of Greenhouse Gas Control*, 90 (66), 102814.
- Fernández J., 2022. Process Simulations and Experimental Studies of  $\text{CO}_2$  Capture. *Energies*, 15, 1-3.
- Hagarová, M., Vaško, M., Pástor, M., Baranová, G., Matvija, M., 2021. Effect of flue gases' corrosive components on the degradation process of evaporator tubes. *Materials*, 14, 1-16.
- Hua Y., Barker R., Neville A., 2015. Comparison of corrosion behaviour for X-65 carbon steel in supercritical  $\text{CO}_2$ -saturated water and water-saturated/unsaturated supercritical. *Journal of Supercritical Fluids*, 97, 224–237.
- Li S., Zhang K., Wang Q., 2019. Experimental study on the corrosion of a downhole string under flue gas injection conditions. *Energy Science and Engineering*, 00, 1-13.
- Meng B., Wang J., Yang L., Zhu L., Chen M., Zhu S., & Wang, F., 2022. Influence of fuel combustion on the corrosion behaviour of pipeline steels in fire flooding technology. *Npj Materials Degradation*, 6(1), 1-9.
- Moreno J., Santos L., Orozco J., Ariza, C., Muñoz S., Peña D., 2021. Determination of corrosion products for steam and flue gas injection environments in a Colombian field by using thermodynamic simulation with HSC Chemistry software. *Journal of Physics: Conference Series*, 1938, 1-7.
- Nikitasari A., Royani A., Priyotomo G., Sundjono., 2021. The effect of flow rate and temperature on corrosion rate of carbon steel pipe in condensate solution from geothermal power plant. *Acta Metallurgica Slovaca*, 27(3), 133-138.
- Orozco J, Kafarov V, Peña D., 2018. Methodology for the Analysis of ASTM A335 P92 Steel Exposed to Real Atmospheres of Refinery Combustion. *Chemical Engineering Transactions* 70 163-168.
- Qing A., Bian C., Ming Z., Han X., Zhang J., 2018. Flow dependence of steel corrosion in supercritical  $\text{CO}_2$  environments with different water concentrations. *Corrosion Science*, 134, 149–161.
- Souza A., da Rocha J., Ponciano G., Palermo L., Mansur C., 2020. Development and application of a passion fruit seed oil microemulsion as corrosion inhibitor of P110 carbon steel in  $\text{CO}_2$ -saturated brine. *Colloids and Surfaces A: Physicochemical and Engineering Aspects*, 599, 1-14.